Landslide Susceptibility Mapping Utilizing the Weighted Frequency Ratio Technique: A Case Study of Klang Valley, Malaysia

Yatim Mustapa, M. F.[1] and Tahar, K. N.[2*]
School of Geomatics Science and Natural Resources, College of Built Environment, Universiti Teknologi MARA, 40450 Shah Alam, Selangor, Malaysia E-mail: mfazuli@gmail.com, khairul0127@uitm.edu.my*
**Corresponding Author*

DOI: https://doi.org/10.52939/ijg.v21i2.3939

Abstract
The escalating impacts of climate change have intensified slope instability and increased landslide occurrences in the rapidly urbanizing Klang Valley, Malaysia. With more intense rainfall and rising temperatures, the region faces unprecedented challenges to soil and slope stability due to rapid urbanization. This study evaluates landslide susceptibility by analyzing rainfall and temperature as primary triggering factors, alongside parameters such as elevation, slope angle, aspect, curvature, lithology, land use, soil properties, and NDVI. Key findings highlight that land use, particularly in commercial, industrial, and infrastructure areas with high FR (9.44) and LSI (2.627), significantly influences landslide susceptibility due to construction and terrain alterations. Steep slopes are especially vulnerable as they accelerate runoff, while areas with low NDVI, indicative of sparse vegetation, are more prone to slope failures due to the stabilizing role of vegetation. Regions characterized by vein quartz (FR=6.31; LSI=0.801), known for its brittle structure, and mined lands disturbed by human activities, also exhibit heightened geological vulnerabilities. Utilizing bivariate regression and the Weighted Frequency Ratio (WFR) method in ArcGIS, the study integrates high-resolution LiDAR and digital terrain models (DTMs) to develop a detailed and accurate landslide susceptibility map. These findings offer critical insights for disaster risk reduction strategies and climate-resilient urban planning in the Klang Valley, aligning with United Nations Sustainable Development Goal (SDG) 13.

Keywords: Frequency Ratio, Geospatial Technology, GIS, Landslide, Susceptibility Mapping

1. Introduction

Slope failures and landslides present significant risks to human life, infrastructure, the environment, and the economy, underscoring the importance of understanding the factors influencing their occurrence and susceptibility, particularly in the context of changing climate conditions. A slope failure is a broader term that encompasses any downward movement of soil or rock on a slope, which may occur gradually or suddenly. In contrast, landslide is defined as the rapid movement of rock, earth, or debris down a slope, typically triggered by gravity and exacerbated by factors such as heavy rainfall, temperature or human activities. Understanding the dynamics of these phenomena is critical for effective risk assessment and management. This study focuses on landslides and aims to evaluate various parameters correlated with rainfall and temperature that influence landslides and slope failures using geospatial techniques. This study identifies rainfall and temperature as primary external factors triggering landslides and slope failures. Additional parameters, influenced by these external factors, include elevation, slope angle, aspect, curvature, lithology, land use, soil properties, and the Normalized Difference Vegetation Index (NDVI) [1] and [2]. The relationships among these parameters will be assessed using the regression and frequency ratio model [2] and [3].

An analysis of the history of landslides in the Klang Valley, including the study area located in Gombak, eastern Selangor, under the administrative purview of Majlis Perbandaran Selayang (MPS), reveals a concerning trend. Over a 28-year period from 1993 to 2021, there have been more than 43 documented cases of landslides, averaging approximately 1.5 incidents per year [4] and [5].

This historical data emphasizes the urgency and significance of studying and addressing the risks associated with these natural hazards [6] and [7]. The impacts of landslides incidents extend across various dimensions, affecting human lives, infrastructure, the environment, the economy, as well as social and community structures. These events can result in loss of life, damage to buildings and roads, disruption of ecosystems, economic losses, and social upheaval within communities [8]. Understanding the full extent of these impacts is crucial for developing effective risk reduction strategies and enhancing overall resilience. To conduct a comprehensive assessment of landslides susceptibility in the study area, a diverse set of data sources was utilized, as outline in Table 1. By integrating these datasets and information, the study develops a comprehensive understanding of the factors influencing landslides susceptibility in the area [1] and [9]. Consequently, this integrated approach can inform effective strategies for mitigating the risks associated with landslides and slope failures [10].

Recent advancements in geospatial technologies and modelling approaches have significantly improved our ability to assess landslide susceptibility and hazards. Research such as [10] have highlighted the utility of Global Climate Models and satellite-based precipitation estimates in characterizing landslide hazards over time scales influenced by climate change. Similarly, research by [6] has demonstrated the effectiveness of GIS-based spatial multicriteria approaches in mapping landslide susceptibility, emphasizing the importance of such methodologies in understanding and mitigating landslide risks.

Furthermore, the research of [11] on the Landslide Awareness System (LAwS) emphasizes the importance of developing proactive systems to manage landslide risks along critical infrastructure corridors, highlighting the role of geotechnical engineering and geology in enhancing safety and resilience. These studies collectively contribute to the body of knowledge an improving landslide risk assessment and management practices. In the context of the study area in Gombak, Selangor, this study intends to build upon existing knowledge and methodologies to develop a tailored approach for assessing landslide susceptibility under changing climate parameters. By leveraging geospatial techniques and a multidisciplinary dataset encompassing various environmental parameters, the study seeks to provide insights that can inform effective risk reduction strategies and enhance the overall resilience of the region to landslide hazards.

2. Study Area, Material and Methods

2.1 Study Area

The Klang Valley, spanning approximately 2,832 km² and encompassing Selangor and Kuala Lumpur, is among the most rapidly urbanizing regions in Malaysia, followed by Penang in the north and Johor Bahru in the south of Peninsular Malaysia. It comprises Kuala Lumpur, Gombak, Hulu Langat, Kuala Langat, Sepang, Klang, and Petaling. This study focuses on Selayang, located within the Gombak region under the purview of Majlis Perbandaran Selayang (MPS) in eastern Selangor (3.26901°N, 101.67856°E) (Figure 1). Selayang covers about 549.33 km², with the focus area being study is 227 km². The region features diverse geology including limestone, slate, phyllite, sandstone and vein quartz and is characterized by uneven, hilly terrain. This geographical landscape makes the area particularly susceptible to landslides, especially in proximity to key infrastructure like Batu Dam and the Sg. Batu Water Treatment Plant. According to the 2010 census, MPS had a population of around 542,409, with projections nearing one million by 2030, resulting in an estimated population density of 1,900 people per km². The rapid urban development, strategic location, excessive rainfall, exceeding 3,000 mm per year [9], was recorded over the past 10 years (2013–2023) and vulnerability to landslides make Selayang a significant focus for the study of landslide susceptibility.

2.2 Material and Methods

In this study, geospatial techniques were applied using the Frequency Ratio (FR) model to analyze landslide susceptibility. Potential and availability of parameters which influencing landslides were assessed geospatially, with regression analysis (R^2) employed to examine their relationships in the first place. Geotechnical input was incorporated to refine the weighted assigned to each factor, enhancing the accuracy of the susceptibility index. The results were then modelled to develop a susceptibility index, classifying areas based on their landslide risk potential, ranging from high to low. The application of advanced geospatial techniques to generate susceptibility maps contributing to inform risk reduction strategies and decision-making processes [10]. The research methodology for assessing landslide and slope failure susceptibility followed a systematic approach involving data inventory, preparation, processing, analysis, interpretation and result, as outlined in Figure 2. Table 1 details the data used and their respective sources.

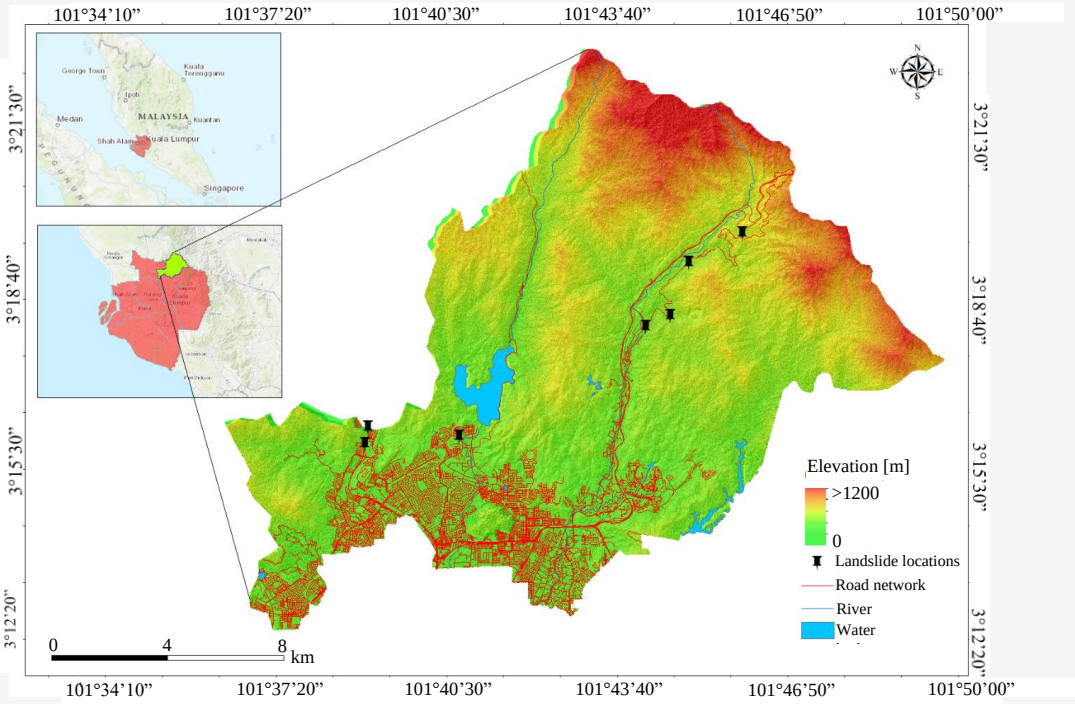

Figure 1: Klang Valley

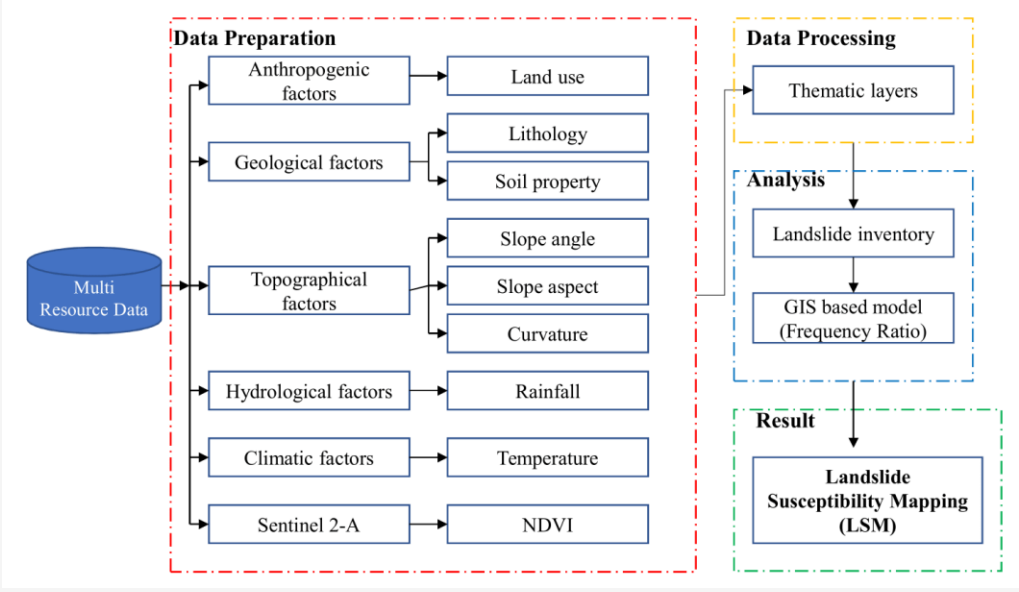

Figure 2: Landslide susceptibility mapping study workflow

2.2.1 Data preparation

In the data preparation phase, both primary and secondary data are collected and categorized to evaluate the factors influencing slope stability and landslide susceptibility in the study area located in Gombak, Selangor, under the administrative purview of Majlis Perbandaran Selayang (MPS) [6]. Data preparation involves the systematic collection and categorization of both primary and secondary data, essential for assessing landslide and slope failure susceptibility. Primary data sources, such as LiDAR, are used to create detailed Digital Terrain Models (DTM) for extracting topographical features like slope angle, aspect, and curvature, which are essential for understanding terrain characteristics and stability [7]. In this study, high-resolution LiDAR data with a 3-meters spatial resolutions is utilized.

Table 1: The list of parameters and data sources used for the study

No.	Parameter	Data/ Format	Scale/ Resolution	Data Availability/Source
1	Rainfall	Tabular	-	Department of Irrigation & Drainage Department of Meteorological, Malaysia
2	Temperature	Tabular	-	Department of Meteorological, Malaysia
3	Slope	Spatial	3 m	LiDAR
4	Aspect	Spatial	3 m	LiDAR
5	Curvature	Spatial	3 m	LiDAR
6	NDVI	Satellite imagery	20 m	Sentinel – 2A, https://www.copernicus.eu/en/access-data
7	Land Use	Spatial	1:200,000	Department of Town & Country Planning, Selangor
8	Soil Property	Spatial	1:20,000	Department of Agriculture, Malaysia
9	Lithology	Spatial	1:200,000	Department of Mineral & Geoscience, Malaysia

Table 2: The Regression analysis (R^2) of causative correlation parameters for rainfall and temperature with landslide susceptibility

Parameter	R^2
Rainfall	0.96
Temperature	0.90

Additionally, secondary data including rainfall data from Department of Irrigation and Drainage, Malaysia, temperature data from Department of Meteorological, Malaysia, soil properties from Department of Agriculture, Malaysia, lithology data from Department of Mineral and Geoscience, Malaysia, land use data from Department of Town & Country Planning, Selangor, and Normalized Difference Vegetation Index (NDVI) from Sentinel 2A satellite imagery are integrated to provide a comprehensive dataset for analysis [8]. Rainfall and temperature are key climate parameters that significantly impact the environment [5]. These parameters have been selected due to the Klang Valley's experience of intense rainfall and temperature variations over the past few years [1][4] [5] and [9]. Additionally, relevant agencies in Malaysia provide this data in tabular format, making it accessible for analysis. Changes in rainfall and temperature lead to variations in vegetation cover (NDVI) [2][12] and [13] soil stability, and other geological properties, ultimately impacting slope stability and landslide risk. This study reveals a strong relationship between rainfall and temperature with other parameters, as indicated by the regression results presented in the Table 2.

2.2.2 Data processing

In the data processing phase, the objective is to prepare all data listed in Table 1 into raster format, ensuring thematic layers are ready for subsequent analysis. Techniques such as interpolation of point data are employed to create continuous distribution surface maps for variables like rainfall (Figure 4(d)) and temperature (Figure 4(e)) using the method of Inverse Distance Weighting (IDW), [14]. IDW is favoured for its simplicity and intuitive approach to estimating values based on the proximity of known data points. The IDW prediction values can be calculated using Equation 1.

$$v' = \frac{\sum_{i=1}^{n} \frac{v_i}{d_i^p}}{\sum_{i=1}^{n} \frac{1}{d_i^p}}$$

Equation 1

Where:

v' = Interpolate value at the location of interest
n = Total number of known location
v_i = Observed value at the i -th known location
d_i = Distance from the prediction location to the i^{th} known location
p = Power parameter controlling the rate at which the influence of distant points diminishes. ($p = 2$)

Additionally, image analysis is performed to calculate NDVI (Figure 4(i)). Prior to this, cloud cover removal using raster function techniques in ArcGIS are applied to enhance imagery clarity, accuracy and visibility, as NDVI serves as a critical indicator of vegetation health.

This process utilizes specific band ratios derived from Sentinel-2A satellite imagery [2] and [15]. The bands considered in the formula are Band 4 (Red) and Band 8 (Near-Infrared) [16]. NDVI from Sentinel-2A is computed using the formula in the Equation 2:

$$NDVI = \frac{NIR - RED}{NIR + RED}$$

Equation 2

Where:

NDVI: Normalized Difference Vegetation Index
NIR: Spectral reflectance acquired from Near-infrared region
RED: Spectral reflectance acquired from Red region

Reclassification is a fundamental process in geospatial analysis for landslide susceptibility studies. It plays a crucial role in simplifying, standardizing, visualizing, and integrating data to enhance clarity and interpretability [1]. By reclassifying parameters such as elevation, slope angle (Figure 4(a)), aspect (Figure 4(b)), and curvature (Figure 4(c)) into discrete classes, researchers can effectively assess landslide susceptibility and apply weighting factors in models like the frequency ratio model [1] and [17]. The landslide susceptibility index can be determined from Equation 3:

$$LSI = \sum_{i=1}^{n} w_i FR_{ij}$$

Equation 3

Where:

LSI = Landslide susceptibility index
n = Number of contributing parameters used in the analysis
w_i = Weighted assigned to the i^{th} parameters
FR_{ij} = The frequency ratio for the j class of the specific parameter i^{th}

Reclassification transforms continuous data into categorical variables, enabling the identification of patterns and trends contributing to landslide occurrence [16]. This process assists in the ranking of features based on their contributions to the study, making it a vital tool in landslide susceptibility assessment [18]. Similarly, map algebra (raster calculator) supports advanced geospatial analysis by performing spatial operations, integrating multiple raster datasets, and combining weighted layer [19]. On the other hand, soil properties (Figure 4(f)) at a scale of 1:20,000, lithology (Figure 4(g)) at a scale of 1:200,000, and land use (Figure 4(h)) at a scale of 1:200,000 are readily available as spatial feature class datasets sourced from relevant agencies as open data. However, strategic site validation is essential to ensure the data's continued relevance and accuracy.

3. Data Analysis

In the analysis phase, bivariate regression is used to examine the correlation between rainfall, temperature, and their contribution to landslides, along with additional factors such as soil properties, digital terrain model (DTM) attributes, slope, aspect, lithology, and NDVI [20]. Table 2 presents the highest regression results achieved in this study, while Figure 3 displays the regression graphs quantifying the correlations with landslide susceptibility. The analysis provides coefficients that measure the strength of each relationship, along with the coefficient of determination (R^2), which indicates the proportion of variance in landslide susceptibility explained by the rainfall and temperature parameters [21]. Rainfall and temperature data were derived from archived records spanning a 10-year period, from 2013 to 2023.

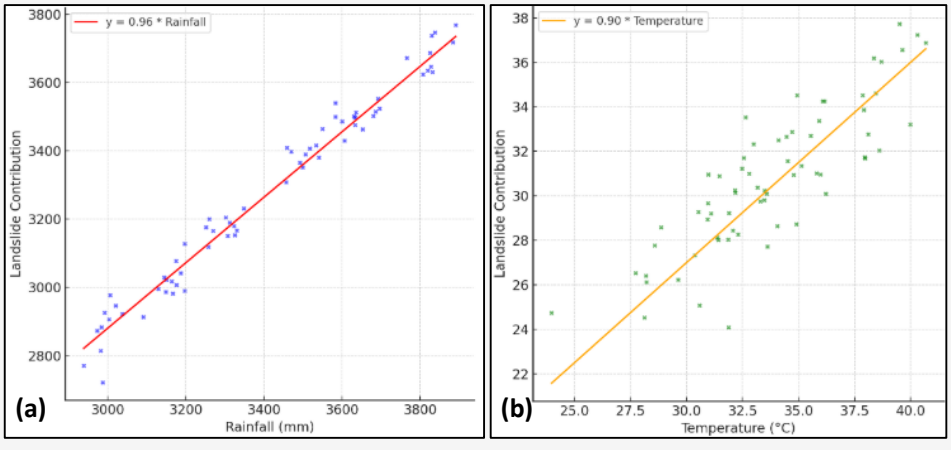

Figure 3: Landslide correlation with (a) rainfall (b) temperature

3.1 Weighted by Ranking Technique

Landslide susceptibility was assessed using a ranking-based weighting technique for all influencing parameters. Given that only nine parameters were involved, the ranking method was chosen for its simplicity in assigning criteria weights, as outlined in [22]. In general, the parameters are ranked based on their significance, from highest to lowest impact parameters into the study area. In addition, these weighting can be calculated using three approaches: rank sum, rank exponent, and rank reciprocal [22]. Among these, the rank sum method was adopted, as shown in Equation 4. According to [23], the weight (W_j) represents the relative importance of each parameter (e.g., slope angle, soil properties, and lithology), while the rating reflects the relative significance of classes within a single parameter (e.g., slope angles of <15° and 15–25°). In this study, the ratings were determined using the frequency ratio index, and the factor weights were computed using the rank sum technique, which involves summing the frequency ratio values for each class of the parameters. The details are provided in Table 3, with the weights (W_j) derived from Equation 4.

$$W_j = \frac{n - p_j + 1}{\sum_{j=1}^{n}\left(n - p_j + 1\right)}$$

Equation 4

Where:

W_j = the weighted of rank sum for the j^{th}

p_j = The rank of the jth for the parameter (lower rank number indicate higher importance)

n = The total number of parameters

Based on Equation 4, the derived weights are presented in Table 3. Among the seven parameters evaluated, land use exhibited the highest weight (0.250), while curvature recorded the lowest (0.036). The frequency ratio analysis indicates that most landslides occur in areas categorized under land use, with commercial, industrial, and transportation classes contributing the most. Detailed contributions of each parameter to landslide susceptibility are provided in Table 4. These weights establish a ranking of parameter importance, emphasizing the role of rainfall and temperature as the primary triggering factors.

3.2 Weighted of Frequency Ratio

In the field of landslide susceptibility mapping, various methodologies have been investigated to enhance predictive accuracy. For example, [24] compared the Random Forest and Frequency Ratio models for landslide susceptibility in Yunyang County, China, emphasizing the need to account for multiple conditioning factors. Similarly, [2] evaluated the Weight of Evidence, Frequency Ratio, and Information Value methods for soil susceptibility in Murree, Pakistan, demonstrating the utility of diverse analytical approaches. [25] further highlighted the importance of integrating geospatial analysis and earth observation data to assess the combined impact of physical and anthropogenic factors on landslides. This study employs the Weighted Frequency Ratio (WFR) method to develop a landslide susceptibility map. The frequency ratio is a straightforward statistical method that effectively captures the linear relationship between landslide distribution and influencing factors, delivering accurate and reliable results [23]. It is widely recognized as one of the most robust GIS-based models for analyzing spatial relationships between variables [2]. This approach evaluates landslide occurrences relative to the total study area, applying weights to factors based on their predictive strength [2] and [26]. The locations of past landslide events in this study area are indicated in Figure 4. The WFR method was implemented in ArcGIS.

Table 3: Rank sum weighted technique for landslide susceptibility

Parameter	Straight rank	Ranking	Rank sum weight (W_j)
Slope angle	5	3	0.107
Slope aspect	2	6	0.214
Curvature	7	1	0.036
Soil property	3	5	0.179
Lithology	4	4	0.143
Land use	1	7	0.250
NDVI	6	2	0.071
Total		28	1.000

Table 4: Ratings of parameters and frequency ratios for each class

Parameter	Class	Number of Pixels in Class	Number of Pixel in Class (%)	Number of Landslide Pixel in Class	Number of Landslide Pixel in Class (%)	Frequency Ratio (FRi)	Sum FRi	Weighted (normalized)	LSI (Value)
Slope Angle	<15°	5080.30	22.3%	1016.06	20%	0.90	6.50	0.107	0.096
	15-25°	6908.99	30.3%	1727.25	25%	0.82			0.088
	25-35°	9391.33	41.2%	2817.40	30%	0.73			0.078
	>35°	1405.65	6.2%	351.41	25%	4.05			0.434
Slope Aspect	F	0	0.0%	0.00	0%	0	19.93	0.214	0.000
	NE	230.09	1.0%	11.50	5%	4.95			1.061
	E	2176.58	9.5%	652.98	30%	3.14			0.673
	SE	8372.86	36.7%	1842.03	22%	0.60			0.128
	S	8858.66	38.9%	885.87	10%	0.26			0.055
	SW	2000.46	8.8%	200.05	10%	1.14			0.244
	W	238.14	1.0%	11.91	5%	4.79			1.025
	NW	126.18	0.6%	2.52	2%	3.61			0.774
	N	789.46	3.5%	39.47	5%	1.44			0.309
Curvature	Concave	12274.91	53.9%	6137.46	50%	0.93	2.71	0.036	0.033
	Flat	702.95	3.1%	21.09	3%	0.97			0.035
	Convex	9808.40	43.0%	3432.94	35%	0.81			0.029
Soil Properties	Mined land	100.89	0.4%	2.02	2%	4.48	9.55	0.179	0.799
	Riverine Alluvial Soils	835.97	3.7%	41.80	5%	1.35			0.241
	Sedentary Soil	18462.07	81.8%	11077.24	60%	0.73			0.131
	Urban Lands	2877.81	12.7%	287.78	10%	0.78			0.140
	Water Bodies	306.77	1.4%	9.20	3%	2.21			0.394
Lithology	Acid Intrusives	18324.15	80.4%	12826.90	70%	0.87	9.49	0.143	0.124
	Limestone/Marble	936.46	4.1%	0.00	0%	0.00			0.000
	Schist	384.94	1.7%	0.00	0%	0.00			0.000
	Phyllite/Slate	2960.08	13.0%	888.02	30%	2.31			0.330
	Vein Quartz	180.63	0.8%	9.03	5%	6.31			0.901
Land Use	Agriculture/Vegetation	868.48	3.8%	26.05	3%	0.79	20.80	0.250	0.198
	Commercial/Industry/Infrastructure	969.43	4.2%	387.77	40%	9.44			2.360
	Housing/Community	1502.44	6.6%	450.73	30%	4.57			1.142
	Forest	16965.98	74.2%	2544.90	15%	0.20			0.051
	Recreational	771.16	3.4%	15.42	2%	0.59			0.148
	Transportation	1541.14	6.7%	77.06	5%	0.74			0.186
	Water Bodies	256.18	1.1%	12.81	5%	4.46			1.116
NDVI	Low	2059.78	9.0%	823.91	40%	4.42	5.74	0.071	0.316
	Medium	4107.78	18.0%	821.56	20%	1.11			0.079
	High	16616.85	72.9%	2492.53	15%	0.21			0.015

This method ensures the analysis is both statistically sound and grounded in practical knowledge, thereby enhancing the reliability and overall robustness of our susceptibility assessments. This approach will be applied to all parameters, including slope, aspect, curvature, soil property, lithology and land use. The raster thematic layers were reclassified and combined using the raster calculator, resulting in a susceptibility map as depicted in Figure 7, categorized into five indices: very high, high, moderate, low, and very low. This method effectively integrates multiple factors to provide a detailed risk assessment for the study area. The FR is defined in Equation 5.

$$FR_i = \frac{N_i p_x / N}{N_i I_p / NI}$$

Equation 4

Where:

F_{Ri} = The Frequency Ratio for the ith class of specific parameter

$N_i p_x$ = The number of pixels with landslide for each parameter

N = The number of total landslide

$N_i I_p$ = The number of pixels in class area

NI = The number of total pixel in study area

This study found a robust relationship between rainfall and the land use which recorded sum of FR cumulative to 20.8, indicating a strong correlation between these variables in influencing landslide susceptibility [10]. The susceptibility map produced from this analysis offers a comprehensive visualization of landslide risk areas within the study region. By integrating advanced statistical methods and geospatial techniques, the map provides valuable insights into the spatial distribution of susceptibility factors, highlighting regions at elevated risk based on rainfall patterns in tropical climate [7]. This approach not only enhances the accuracy of landslide risk assessments but also supports targeted mitigation efforts by identifying critical areas prone to landslides [16].

4. Results

4.1 Landslide Influencing Factors

The inventory map in Figure 4, generated from previous processing stages, classifies each dataset into standard classes based on specific parameters such as elevation (DTM), slope angle, rainfall, temperature, slope aspect, curvature, NDVI, soil properties, land use, and lithology. This detailed categorization of the study area's characteristics facilitates a more nuanced understanding of the environmental factors influencing landslide and slope failure susceptibility [1] and [9]. The classification is based on previous research and incorporates insights from local geologists familiar with the study environment [2] and [27].

4.1.1 Elevation

In landslide susceptibility study, environmental parameters are classified into standard categories as indicate by previous researcher to facilitate analysis and modelling, offering insights into factors contributing to landslide risk. The Figure 1 illustrates the Digital Terrain Models (DTMs), derived from LiDAR data, which beneficial for assessing landslide susceptibility by provide accurate topographic information for analyzing and predicting landslide-prone areas [28]. Details of the LiDAR data are outlined in Table 1. The 3-meter spatial resolution of LiDAR has demonstrated its effectiveness in enabling quantitative analyses of topographic and geomorphological processes [23] and [28].

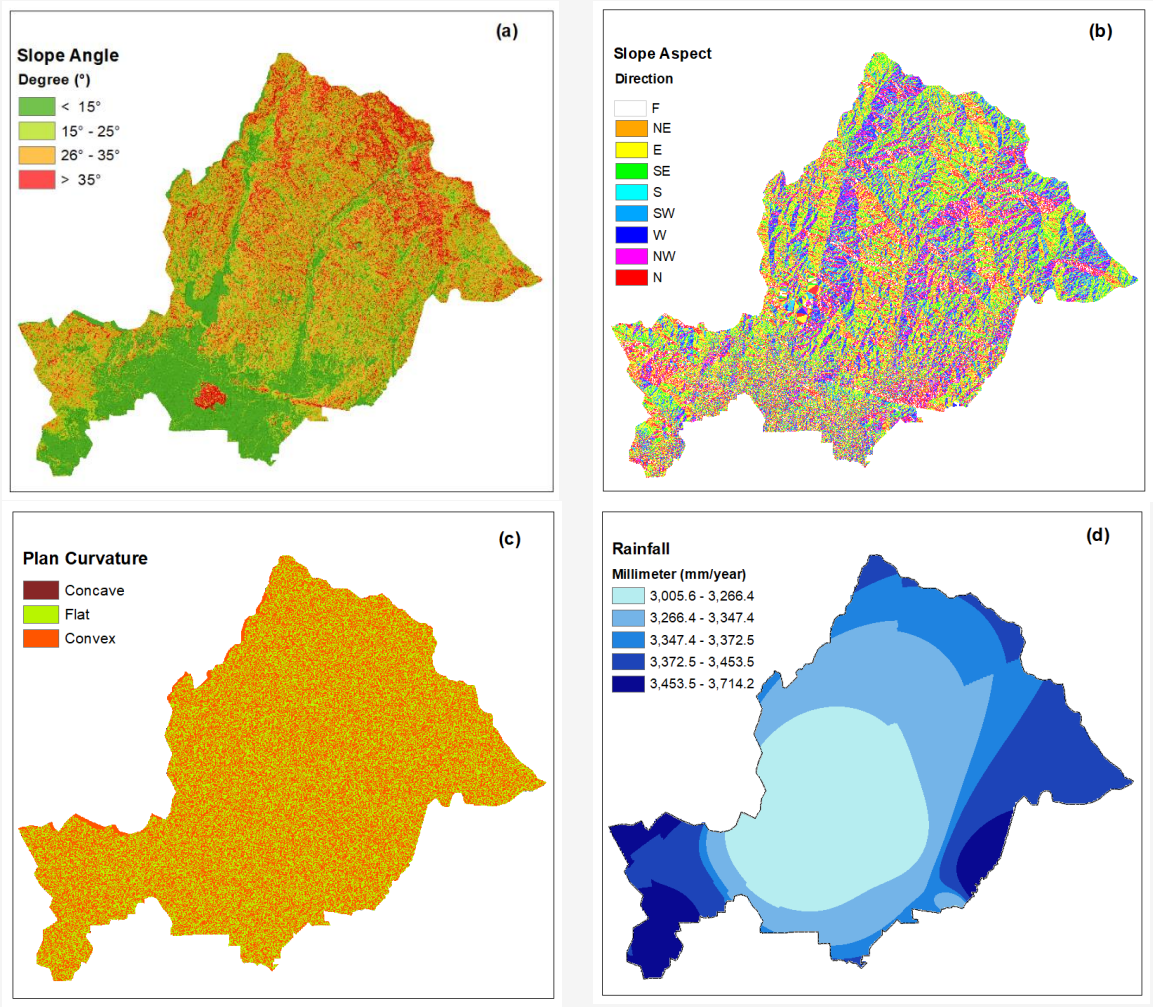

Figure 4: Landslide influencing factors:
(a) slope angle, (b) slope aspect, (c) curvature, (d) rainfall
(Continue next page)

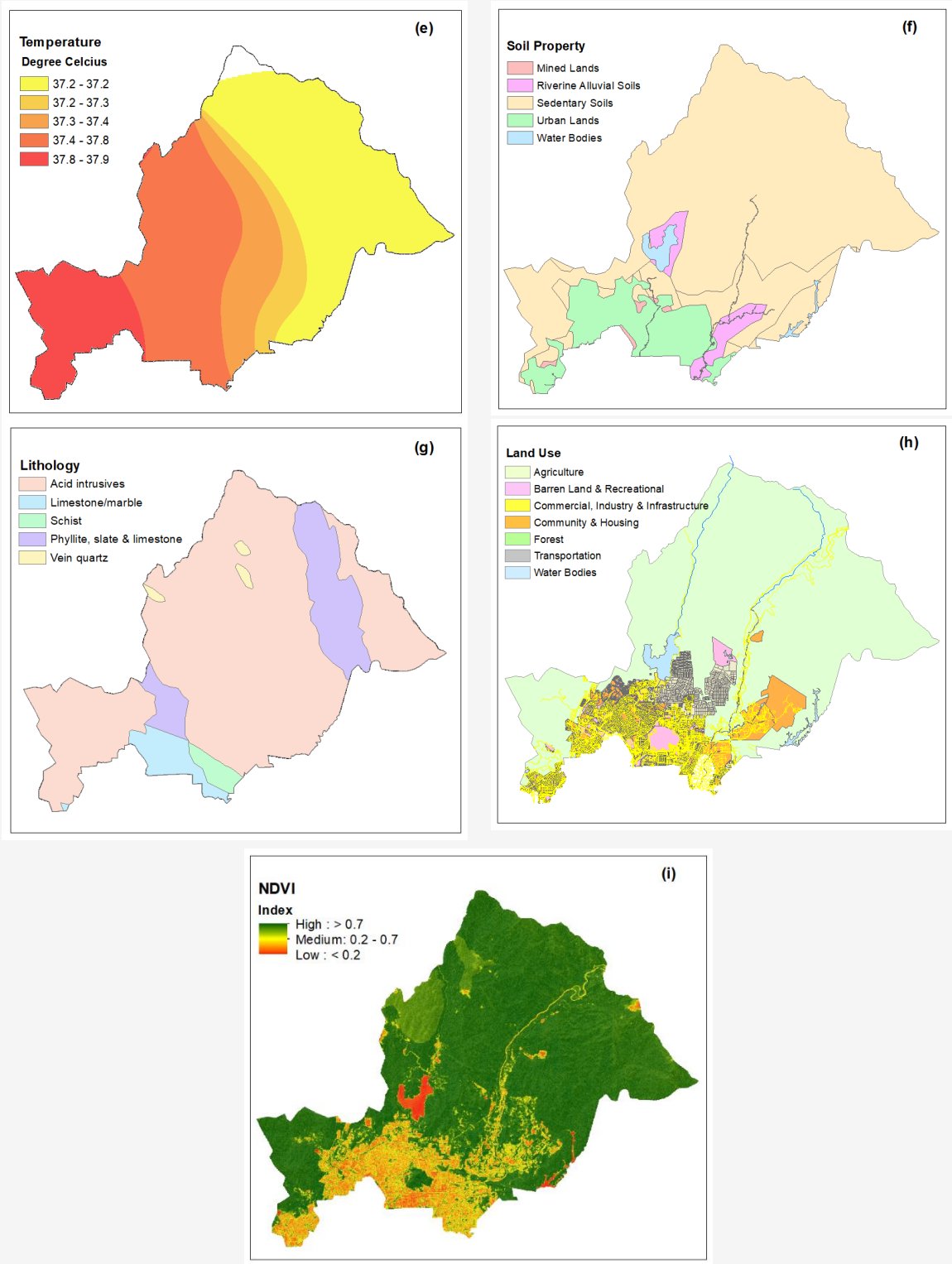

Figure 4: Landslide influencing factors:
(e) temperature, (f) soil property (g) lithology, (h) land use, and (i) NDVI
(Continue from previous page)

4.1.2 Slope angle

Slope angle play a crucial role in evaluating landslide failure susceptibility especially within Klang Valley distinctive terrain. Figure 4(a) describes the slope angle, which is categorized into four classes [5]: gentle slopes (<15°) cover 22.3% of the area and represent relatively stable regions with lower landslide risk; moderate slopes (15°-20°) cover 30.32% of the area and are associated with a slightly higher risk; steep slopes (25°-35°) cover 41.21% of the area and are high-risk areas for landslides; and very steep slopes (>35°) cover 6.17% of the area and represent the highest risk areas [1] [9] and [28]. This categorization was established and governed by the relevant Malaysia's government agency responsible pertaining to the slope.

4.1.3 Aspect

The orientation of a slope, known as slope aspect, stands as a critical factor in evaluating the susceptibility of slope failures. The aspect of a slope plays a technical role in shaping its potential for instability. The Figure 4(b) illustrates slope aspect, which refers to the compass direction a slope faces and its effect on the amount of sunlight it receives. This, in turn, influences factors such as soil moisture, vegetation health, and other environmental conditions [14] and [28]. In geospatial analysis, slope aspect is typically classified into nine categories [2]: North, Northeast, East, Southeast, South, Southwest, West, Northwest, and Flat. In Peninsular Malaysia, southern-facing slopes (157°–202°) receive more sun exposure due to the region's geographical orientation, while northern-facing slopes (0°–22° and 337°–360°) receive significantly less sunlight. Referring to Table 4, it is recorded that the Northeast (NE), East (E), West (W), Northwest (NW), and North (N) categories show WFR values greater than 1.

4.1.4 Curvature

Figure 4(c) shows curvature, which is another critical parameter contribute to landslide susceptibility. Convex hillsides generally have greater stability compared to concave hillsides. In contrast, concave hillsides tend to be more unstable due to the accumulation of water at the lowest point of the slope, which increases hydrostatic pressure [3]. In this area of study, concave areas, which cover 56.63% of the study area, are likely to accumulate water and debris, increasing landslide risk [2] and [3]. Convex areas, covering 43.05% of the region, typically shed water and debris, reducing landslide risk [2], while flat areas, covering 0.32%, are relatively stable.

4.1.5 Rainfall

Heavy rainfall increases the risk of landslide failure by saturating the soil, raising pore water pressure, and reducing cohesion, which weakens the slope's stability [1] and [2]. The added weight of water can also trigger failure if it exceeds the soil's strength, especially in already unstable areas [29]. Rainfall (Figure 4(d)) is classified into five categories very low, low, moderate, high, and very high reflecting its role in landslide susceptibility. These categories are key factors in this study. Intense rainfall, over 3000 mm annually or in short bursts, can cause erosion, removing protective soil and vegetation [9]. In areas with a high water table, heavy rain can increase pressure on the slope's base, reducing stability [28]. Additionally, changing rainfall patterns due to climate change require a better understanding for effective risk management. Rainfall (Figure 4(d)), classified into five categories very low, low, moderate, high, and very high reflecting the climatic conditions that contribute to landslide susceptibility. These parameters serve as causal factors in this study.

4.1.6 Temperature

In tropical countries, temperature changes play a key role in slope failure due to the region's climate. Clay-rich soils expand during the rainy season and shrink in hot, dry periods, which can stress the slope and cause instability [30]. Temperature (Figure 4(e)) is classified into five categories very low, low, moderate, high, and very high reflecting how climate affects landslide risk. These categories are key factors in this study. Daily temperature variations can also cause rocks and soils to crack, weakening the slope. Intense heat can dry soils, reducing cohesion and increasing erosion and sliding. Additionally, high temperatures can weaken vegetation, reducing root cohesion and further destabilizing slopes [1].

4.1.7 Soil property

Malaysia's landscape features various soil types affecting slope stability. Cohesive clay-rich soils provide stability but are prone to shrink-swell behaviour, while loose granular soils like sand and gravel lack cohesion and are more vulnerable to mass movements, with high silt content increasing landslide risk during heavy rainfall [1]. The variation in composition and moisture content between alluvial and colluvial soils significantly influences slope stability. Peat soils, most likely present in area such as riverine alluvial soil, characterized by their high organic content, exhibit low shear strength, rendering them particularly susceptible to slope failures when saturated, especially during periods of heavy rainfall [2] [14] and [31].

The interplay of these unique soil properties with factors such as rainfall, topography, and land use highlights the inherent complexity of assessing landslide susceptibility in Malaysia. In this study area, soil properties are categorized into five distinct types based on data from the originating agency: mined lands, riverine alluvial soils, sedentary soils, urban lands, and water bodies. Figure 4(f) illustrates the distribution of soil categories and their respective coverage area percentages, arranged from largest to smallest: Sedentary Soils (81.75%), Urban Lands (12.74%), Riverine Alluvial Soils (3.7%), Water Bodies (1.36%), and Mined Lands (0.45%). Each soil type plays a crucial role in determining landslide susceptibility within the region.

4.1.8 Lithology

Lithology is a crucial factor in landslide occurrence, as it influences the strength and permeability of the bedrock, which in turn affects slope stability. Factors such as infiltration rates, soil drainage, and material variability contribute to increased pore pressure, which reduces slope stability [1]. The composition of a slope, including its rock or soil type, is a key factor in its stability. In Malaysia's Klang Valley, as noted by [32] two main lithologies dominate: phyllite and quartzite. Phyllite has high clay (41-60%) and silt (20-45%) content, making it prone to water retention and swelling during heavy rainfall. Quartzite, with higher sand content (37-67%) and lower clay content (6-43%), allows for better drainage, reducing the risk of instability. Hard rocks like granite are generally stable due to their high shear strength, while unconsolidated sediments (e.g., loose soil, gravel) and weak rocks like shale or schist are more susceptible to erosion and landslides [2]. Figure 4(g) classifies the lithology of the study area into five categories and their respective coverage areas, arranged from largest to smallest: acid intrusives (80.42%), phyllite (12.99%), limestone (4.11%), schist (1.7%), and vein quartz (0.8%). These categories are crucial for assessing landslide risk by evaluating the impact of geological composition on slope stability.

4.1.9 Land use

Land Use is a critical factor in assessing slope failure susceptibility, as it highlights the impact of human activities on slope stability. Urbanization, deforestation, and agricultural practices often remove stabilizing vegetation, alter drainage patterns, and increase the risk of slope failures. Understanding the relationship between land use changes and slope stability is essential for evaluating risks from human-induced landscape modifications.

As suggested by [1] that future slope failures are likely to mirror past events due to ongoing instability. In Malaysia, rapid urbanization, agricultural expansion, and deforestation are reshaping the landscape [33], significantly affecting slope stability. Figure 4(h) classifies land use into seven categories, ranked from the largest to smallest coverage area within the study area: Forested Areas (74.17%), Transportation (6.74%), Housing/Community Areas (6.6%),Commercial/Industrial/Infrastructure (4.2%), Agricultural/Vegetation (3.8%), Recreational Areas (3.37%), and Water Bodies (1.12%). Integrating this data into Geographic Information Systems (GIS) is essential for accurate risk assessment and enhances decision-making in urban planning, disaster management, and environmental protection.

4.1.10 NDVI

The Normalized Difference Vegetation Index (NDVI) is crucial for assessing slope failure risk, as it reflects vegetation health and density. Higher NDVI values indicate dense, healthy vegetation that stabilizes slopes by reducing erosion and providing support, while lower values show sparse vegetation, increasing the risk of instability [2]. Figure 4(i) illustrates the NDVI distribution in the study area and its coverage area, arranged from largest to smallest: high NDVI (72.93%), medium NDVI (18.03%), and low NDVI (9.04%), with low NDVI primarily found in urban and commercial areas. NDVI data from Sentinel-2A (2023) is valuable for assessing landslide susceptibility.

4.2 Landslide Susceptibility Zonation

According to [23], the objective of zonation is to delineate study areas based on the Landslide Susceptibility Index (LSI), with mapping achieved through cell values calculated using Equation 3. In this study, the LSI values range from 0.016 to 2.627 and were classified into categories using the ArcGIS quantile break method. Areas with high NDVI values recorded an LSI of 0.016, indicating very low susceptibility to landslides. In contrast, land use categorized as commercial/industrial/infrastructure exhibited very high LSI values (>1), signifying a heightened risk of landslides, particularly during periods of excessive rainfall. By integrating advanced statistical methods and geospatial techniques, this mapping approach provides valuable insights into the spatial distribution of susceptibility factors. It highlights regions at elevated risk based on rainfall patterns and vegetation health, as indicated by NDVI values [7].

This methodology not only enhances the accuracy of landslide risk assessments but also aids in the identification of critical areas that require targeted mitigation efforts. Figures 5 and 6 illustrate the seven archived spot locations within the study area where landslides have occurred, with most incidents happening in infrastructure (road network) areas. Overlaying Figure 7 with the archived landslide locations shows that landslide occurrences at three spot locations (a, b, c, and e) align with high LSI values from the FR model, while the remaining four locations (d, f, and g) show landslide occurrences at very low and low LSI values.

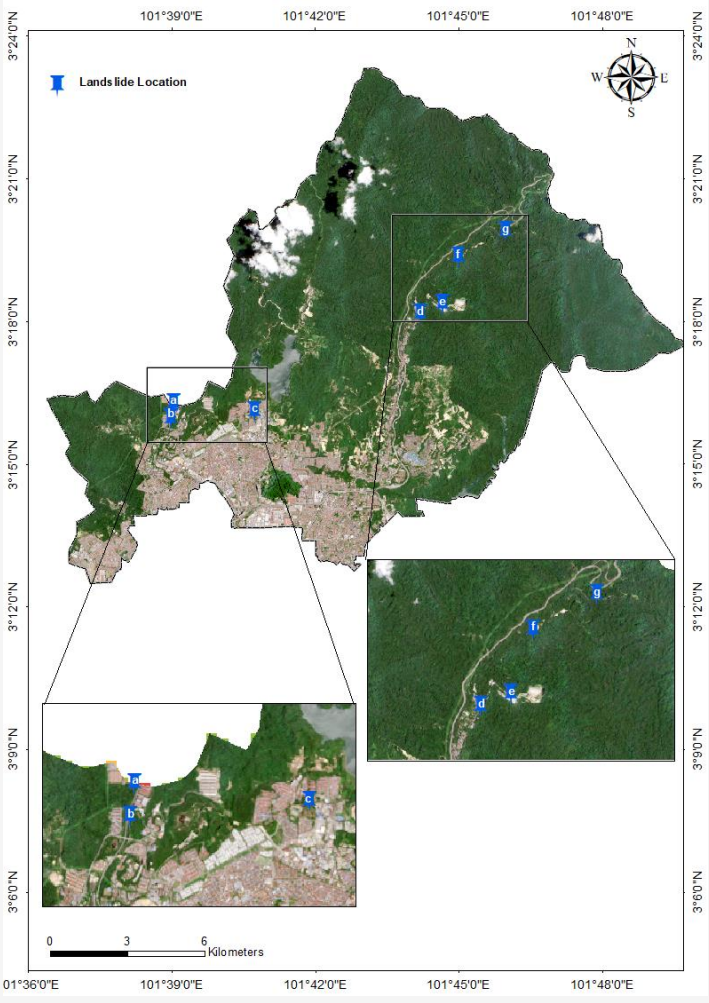

Figure 5: Landslide inventory location in the study area

Table 5: Landslide susceptibility classes generated from the frequency ratio

Susceptibility Classes	**LSI Value**	**Area (km²)**	**Area (%)**
Very low	< 0.1	86.3	37.85
Low	0.1 – 0.3	62.53	27.43
Moderate	0.3 – 0.6	28.52	12.51
High	0.6 – 1.0	37.8	16.58
Very high	> 1.0	12.84	5.63
Total		227.99	100.00

Figure 6: Photographs of landslide inventory locations obtained from archival documents within the MPS purview: (a) Taman Amansiara, Selayang; (b) Jalan Selayang-Templer in 2009; (c) Taman Selayang Permata in 2023; (d, e, f, g) show landslides occurring at various locations along Jalan Gombak Lama – Genting Sempah, some of which have already been repaired

5. Discussion

In this study, nine landslide inventory parameters were analyzed, with two of them rainfall and temperature acting as triggering factors. Studies conducted in similar tropical climates, such as Bogor, Indonesia [1], Ratnagiri, India [9], and Khao Yai, Thailand [14], have highlighted rainfall and temperature as critical causative factors. In the Klang Valley, rainfall data from the past decade (2013–2023) reveals annual precipitation exceeding 3,000 mm, classifying it as excessive rainfall and heightening landslide risk in vulnerable areas as highlighted by [1]. Elevation is widely recognized as a key parameter in landslide susceptibility studies due to its role as a primary input for analyzing slope, aspect, and curvature. High-resolution elevation data is crucial for studying terrain and topography [28]. For this study, a Digital Terrain Model (DTM) with a 3-meter spatial resolution, derived from LiDAR elevation data, was utilized as a primary input. Similarly to the study conducted by [14] in the region of Thailand, where LiDAR played a vital role in providing essential information. All parameters were processed and converted into thematic layers for analysis. The nine thematic layers slope angle, aspect, curvature, rainfall, temperature, soil properties, lithology, land use, and NDVI were classified based on several previous studies, including [1] [2] and [9]. These classifications were tailored to fit the analysis, which employed a weighted sum ranking technique (Table 3) to model the susceptibility map using the frequency ratio method. From Table 4, the highest normalized weight was recorded by the land use parameter (0.250 for the commercial/industrial/infrastructure class), which subsequently contributed to an LSI value of 2.360, indicating a very high risk (>1.0).

Based on Equation 5, the landslide susceptibility map (LSM) was generated, as shown in Figure 7, where five zonation classes very low, low, moderate, high, and very high were established, consistent with previous studies [1][2] and [3] ,as outlined in Table 5. Within the 227.99 km² study area, an estimated 23–25% of the total area falls within the high to very high susceptibility range. These high-risk zones, as depicted in Figure 7, are predominantly associated with land use classes categorized as commercial, industrial, and infrastructure. Notably, seven historical landslide events occurred within these land use classes.

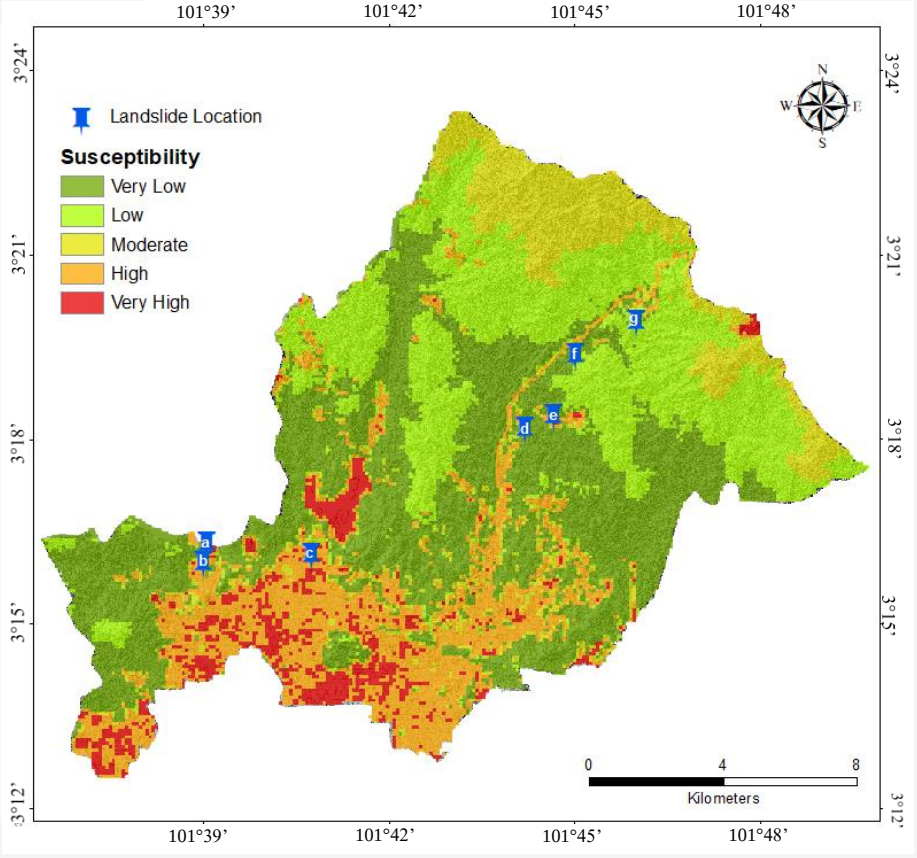

Figure 7: Landslide susceptibility map of Selayang (Klang Valley), Malaysia

The LSM developed in this study accurately identified four out of the seven historical landslide locations (57% - location a, b, c and e) within the high and very high susceptibility categories, demonstrating the model's reliability in capturing landslide-prone areas. Referring to Figure 7, the landslide-prone areas are predominantly located at elevations below 250 m, where rapid urbanization is occurring. This finding is consistent with the study conducted by [1] in the Bogor region of Indonesia, where most landslides also occurred within the same elevation range. For future studies, it is recommended to collect additional and more landslide samples in the study area and employ an artificial neural network (ANN) to validate the model's results, similar to approaches used in [17] and [34]. The primary challenge in this study area is the lack of a centralized, master record for historical landslide data. The information is scattered across various agencies, making it difficult to consolidate. Additionally, some agencies have restrictive information-sharing policies, limiting access to detailed data.

6. Conclusion

This study evaluates landslide susceptibility in the Klang Valley using geospatial techniques and the frequency ratio (FR) model, focusing on key parameters such as rainfall, temperature, elevation, slope angle, aspect, curvature, soil properties, lithology, land use, and NDVI. Nine thematic layers were analyzed to calculate FR values, assign weights, and derive the Landslide Susceptibility Index (LSI) through a weighted formula. The highest FR was recorded for commercial/industrial/infrastructure land use (FR = 9.44), while the lowest was for forested areas (FR = 0.20). Similarly, the highest LSI (LSI > 1) was observed in commercial/industrial areas (LSI = 2.627), indicating significant landslide potential, with 43% of recorded landslide spots occurring in infrastructure areas such as roads. Conversely, areas with high NDVI showed the lowest LSI (0.016), underscoring the stabilizing role of vegetation.

Rainfall and temperature emerged as critical triggering factors, with annual precipitation exceeding 3,000 mm intensifying landslide risks. Steep slopes (>35°) significantly contributed to susceptibility due to gravitational forces, while flatter slopes (<15°) were relatively stable. Slope aspect analysis revealed heightened susceptibility on northeast-facing slopes (FR = 4.95, LSI = 1.321), while curvature analysis identified concave areas as more susceptible (FR = 0.93, LSI = 0.034). Soil properties indicated that mined lands were the most unstable (FR = 4.48, LSI = 0.572), whereas sedentary soils were more stable (FR = 0.73, LSI = 0.094). Lithology analysis showed vein quartz as the most landslide-prone (FR = 6.31, LSI = 0.801), while acid intrusive were more stable (FR = 0.87, LSI = 0.111).Overall, 37.85% of the study area falls into the very low susceptibility class (LSI < 0.1), 27.43% into low susceptibility (LSI 0.1–0.3), 12.51% into moderate susceptibility (LSI 0.3–0.6), 16.58% into high susceptibility (LSI 0.6–1.0), and 5.63% into very high susceptibility (LSI > 1.0). These findings highlight the spatial variation in landslide risk, influenced by both natural and anthropogenic factors.

To enhance the accuracy and reliability of future landslide susceptibility studies, it is recommended to strengthen collaboration with relevant agencies to acquire more accurate and reliable parameter data, particularly rainfall, soil, and lithology information, which are currently challenging to obtain. Additionally, increasing the number of sampled landslide locations will address the limitations posed by the current dataset and provide a more comprehensive representation of landslide occurrences. With access to additional landslide information, larger training and testing datasets can be developed, enabling refined models that reduce uncertainties and improve predictive accuracy. Future studies should also explore the integration of advanced techniques, such as machine learning models and high-resolution remote sensing datasets, to complement traditional FR analysis.

Acknowledgement

This research was financially supported by Universiti Teknologi MARA and the Institute of Postgraduate Studies (IPSis), UiTM. The authors would like to thank the relevant internal and external agencies that contributed to this research, as well as all the industrial experts involved. Special thanks are extended to supervisor for the guidance and to families for their unwavering support.

References

[1] Pamela, F. E. S. S., Arifianti, Y. and Hidayat, F., (2019). Landslide Susceptibility Assessment Using Frequency Ratio Model in Bogor, West Java, Indonesia. *Geoscience Letter*, Vol. 6(1). https://doi.org/10.1186/s40562-019-0140-4.

[2] Islam, F., Ahmad, M. N., Janjuhah, H. T., Ullah, M., Islam, I. U., Kontakiotis, G., Skilodimou, H. D. and Bathrellos, G. D., (2022). Modelling and Mapping of Soil Erosion Susceptibility of Murree, Sub-Himalayas Using GIS and RS-Based Models. *Applied Sciences (Switzerland)*, Vol. 12(23). https://doi.org/10.3390/app122312211.

[3] Jahandar, O., Abdi, E. and Jaafari, A., (2022). Assessment of Slope Failure Susceptibility Along Road Networks in a Forested Region, Northern Iran. *Physics and Chemistry of the Earth*, Vol. 128. https://doi.org/10.1016/j.pce.2022.103272.

[4] Majid, N. A., (2020). Historical Landslide Events in Malaysia 1993-2019. *Indian Journal Science Technology*, Vol. 13(33), 3387–3399. https://doi.org/10.17485/ijst/v13i33.884.

[5] Diana, M. I. N., Muhamad, N., Taha, M. R., Osman, A. and Alam, M. M., (2021). Social Vulnerability Assessment for Landslide Hazards in Malaysia: A Systematic Review Study. *Land (Basel)*, Vol. 10(3). https://doi.org/10.3390/land10030315.

[6] Khuc, T., Truong, X., Tran, V., Bui, D., Bui, D., Ha, H., Tran, T., Pham, T., and Yordanov, V. (2023). Comparison of Multi-Criteria Decision Making, Statistics, and Machine Learning Models for Landslide Susceptibility Mapping in Van Yen District, Yen Bai Province, Vietnam . *International Journal of Geoinformatics*, VOl. 19(7), 33–45. https://doi.org/10.52939/ijg.v19i7.2743..

[7] Emberson, R., Kirschbaum, D. and Stanley, T., (2020). New Global Characterisation of Landslide Exposure. *Natural Hazards and Earth System Science*, Vol. 20(12). https://doi.org/10.5194/nhess-20-3413-2020.

[8] Vega, J., (2023). Landslide Modeling in a Tropical Mountain Basin Using Machine Learning Algorithms and Shapley Additive Explanations. *Air Soil and Water Research*, Vol. 16(1). https://doi.org/10.1177/11786221231195824.

[9] Khuc, T., Truong, X., Tran, V., Bui, D., Bui, D., Ha, H., Tran, T., Pham, T., and Yordanov, V. (2023). Comparison of Multi-Criteria Decision Making, Statistics, and Machine Learning Models for Landslide Susceptibility Mapping in Van Yen District, Yen Bai Province, Vietnam . *International Journal of Geoinformatics*, Vol. 19(7), 33–45. https://doi.org/10.52939/ijg.v19i7.2743.

[10] Kirschbaum, D., Kapnick, S. B., Stanley, T. and Pascale, S., (2020). Changes in Extreme Precipitation and Landslides Over High Mountain Asia. *Geophysical Research Letter*, Vol. 47(4). https://doi.org/10.1029/2019gl085347.

[11] Miele, P., Di Napoli, M., Guerriero, L., Ramondini, M., Sellers, C., Annibali Corona, M. and Di Martire, D., (2021). Landslide Awareness System (LAwS) to Increase the Resilience and Safety of Transport Infrastructure: The Case Study of Pan-American Highway (Cuenca–Ecuador). *Remote Sensing*, Vol. 13(8). https://doi.org/10.3390/rs13081564.

[12] Razali, I. H., Mohd Taib, A., Abd Rahman, N., Abang Hasbollah, D. Z., Md Dan, M. F., Ramli, A.B. and Ibrahim, A., (2022). Slope Stability Analysis of Riverbank in Malaysia with the Effects of Vegetation. *Physics and Chemistry of the Earth*, Vol. 129. https://doi.org/10.1016/j.pce.2022.103334.

[13] Sengani, F., Muavhi, N. and Mulenga, F., (2022). Establishing Reliable Slope Stability Hazard Map Based on GIS-Based Tool in Conjunction with Finite Element Methods. *Advances in Civil Engineering*, Vol. 2022. https://doi.org/10.1155/2022/3384143.

[14] Chaikaew, N., Kumsap, C., Wutthisakkaroon, C. and Pimmasarn, S., (2023). Landslide Susceptibility Mapping Using LiDAR Data: A Case Study of Khao Yai National Park, Thailand. *International Journal of Geoinformatics*, Vol. 19(3), 1–12. https://doi.org/10.52939/ijg.v19i3.2597.

[15] Wang, Y., Sun, D., Wen, H., Zhang, H., and Zhang, F. (2020). Comparison of Random Forest Model and Frequency Ratio Model for Landslide Susceptibility Mapping (LSM) in Yunyang County (Chongqing, China). *International Journal of Environmental Research and Public Health*, Vol. 17(12). https://doi.org/10.3390/ijerph17124206.

[16] Pal, S. C. and Chowdhuri, I., (2019). GIS-Based Spatial Prediction of Landslide Susceptibility Using Frequency Ratio Model of Lachung River Basin, North Sikkim, India. *SN Applied Science*, Vol. 1(5). https://doi.org/10.1007/s42452-019-0422-7.

[17] de Oliveira, G. G., Ruiz, L. F. C., Guasselli, L.A. and Haetinger, C., (2019). Random Forest and Artificial Neural Networks in Landslide Susceptibility Modeling: A Case Study of the Fão River Basin, Southern Brazil. *Natural Hazards*, Vol. 99(2), 1049–1073. https://doi.org/10.1007/s11069-019-03795-x.

[18] Conforti, M. and Ietto, F., (2021). Modeling Shallow Landslide Susceptibility and Assessment of the Relative Importance of Predisposing Factors, through a GIS-Based Statistical Analysis. *Geosciences (Switzerland)*, Vol. 11(8). https://doi.org/10.3390/geosciences 11080333.

[19] Kumne, W., and Samanta, S. (2023). Geospatial Mapping of Inland Flood Susceptibility Based on Multi-Criteria Analysis – A Case Study in the Final Flow of Busu River Basin, Papua New Guinea. *International Journal of Geoinformatics*, Vol. 19(6), 31–48. https://doi.org/10.52939/ijg.v19i6.2693.

[20] Li, Y. and Chen, W., (2019). Landslide Susceptibility Evaluation Using Hybrid Integration of Evidential Belief Function and Machine Learning Techniques. *Water (Basel)*, Vol. 12(1). https://doi.org/10.3390/w12010113.

[21] Batar, A. K. and Watanabe, T., (2021). Landslide Susceptibility Mapping and Assessment Using Geospatial Platforms and Weights of Evidence (WoE) Method in the Indian Himalayan Region: Recent Developments, Gaps, and Future Directions. *ISPRS International Journal of Geo-Information*, Vol. 10(3). https://doi.org/10.3390/ijgi10030114.

[22] Shu, H., Guo, Z., Qi, S., Song, D., Pourghasemi, H. R. and Ma, J., (2021). Integrating Landslide Typology with Weighted Frequency Ratio Model for Landslide Susceptibility Mapping: A Case Study from Lanzhou City of Northwestern China. *Remote Sensing*, Vol. 13(18). https://doi.org/10.3390/rs13183623

[23] Nguyen, D., Chou, T., Hoang, T., and Chen, M. (2023). Flood Susceptibility Mapping Using Machine Learning Algorithms: A Case Study in Huong Khe District, Ha Tinh Province, Vietnam. *International Journal of Geoinformatics*, Vol. 19(7), 1–15. https://doi.org/10.52939/ijg.v19i7.2739.

[24] Liu, S., Yin, K., Zhou, C., Gui, L., Liang, X., Lin, W. and Zhao, B., (2021). Susceptibility Assessment for Landslide Initiated along Power Transmission Lines. *Remote Sensing*, Vol. 13(24). https://doi.org/10.3390/rs13245068.

[25] Pokharel, B., Alvioli, M. and Lim, S., (2021). Assessment of Earthquake-Induced Landslide Inventories and Susceptibility Maps Using Slope Unit-Based Logistic Regression and Geospatial Statistics. *Scientific Report*, Vol. 11. https://doi.org/10.1038/s41598-021-00780-y.

[26] Abdul Rahim, A. F., Simon, N., Mohamed, T. R., Md Rafek, A. G., Serasa, A. S., Chen, Y., Zhang, M., Ern, L. K. and Lai, G.T., (2019). Probabilistic Analysis of Potential Planar-Type Rock Slope Failure of Selected Malaysian Rock Slopes. *Bulletin of the Geological Society of Malaysia*, Vol. 67, 83–90. https://doi.org/10.7186/bgsm67201910.

[27] Okoli, J., Nahazanan, H., Nahas, F., Kalantar, B., Shafri, H. Z. M. and Khuzaimah, Z., (2023). High-Resolution Lidar-Derived DEM for Landslide Susceptibility Assessment Using AHP and Fuzzy Logic in Serdang, Malaysia. *Geosciences*, Vol. 13(2). https://doi.org/10.3390/geosciences13020034

[28] Liu, X., Wang, Y. and Leung, A. K., (2023). Probabilistic Back Analysis of Rainfall-Induced Slope Failure Considering Slope Survival Records from Past Rainfall Events. *Computers and Geotechnics*, Vol. 159. https://doi.org/10.1016/j.compgeo.2023.105436.

[29] Nobahar, M., Salunke, R., Alzeghoul, O. E., Khan, M. S. and Amini, F., (2023). Mapping of Slope Failures on Highway Embankments using Electrical Resistivity Imaging (ERI), Unmanned Aerial Vehicle (UAV), and Finite Element Method (FEM) Numerical Modeling for Forensic Analysis. *Transportation Geotechnics*, Vol. 40. https://doi.org/10.1016/j.trgeo.2023.100949.

[30] De Caires, S. A., St Martin, C., Wuddivira, M. N., Farrick, K. K. and Zebarth, B. J., (2023). Predicting Soil Depth in a Humid Tropical Watershed: A Comparative Analysis of Best-Fit Regression and Geospatial Models. *Catena*, Vol. 222. https://doi.org/10.1016/j.catena.2022.106843.

[31] Ali, A. M. and Mohamad, Z. A., (2021). *Three Slope Failures in Malaysia: Lessons Learned and Suggestions for the Future:* 2022 CGS Conference Update: GeoCalgary 2022, Oct 2-5, 2022, Hyatt Regency Calgary, Calgary, AB.

[32] Rendana, M., Idris, W. M. R., Rahim, S. A., Abdo, H. G., Almohamad, H., Al Dughairi, A. A. and Al-Mutiry, M., (2023). Relationships between Land Use Types and Urban Heat Island Intensity in Hulu Langat District, Selangor, Malaysia. *Ecological Processes*, Vol. 12(33). https://doi.org/10.1186/s13717-023-00446-9.